



Morteza Nazerian<sup>1</sup>, Meysam Kamyabb<sup>2</sup>, Mohammad Shamsianb<sup>3</sup>, Mohammad Dahmardehb<sup>4</sup>, Mojtaba Kooshaa<sup>5</sup>

## COMPARISON OF RESPONSE SURFACE METHODOLOGY (RSM) AND ARTIFICIAL NEURAL NETWORKS (ANN) TOWARD EFFICIENT OPTIMIZATION OF FLEXURAL PROPERTIES OF GYPSUM-BONDED FIBERBOARDS

NAZERIAN, M.; KAMYABB, M.; SHAMSIANB, M.; DAHMARDEHB, M.; KOOSHAA, M. Comparison of response surface methodology (RSM) and artificial neural networks (ANN) towards efficient optimization of flexural properties of gypsum-bonded fiberboards. **CERNE**, v. 24, n. 1, p. 35-47, 2018.

### HIGHLIGHTS

The higher non-wood extractives causes to the higher setting time of the gypsum paste, while temperature decreases.

The ANN prediction model is a quite effective tool for modeling bending strength of gypsum-bonded fiberboard.

Maximum MOR is achieved by increase in bagasse, kenaf and glass fibers content and reaches to 10.81 MPa and 11 MPa by RSM and ANN at optimum condition.

### ABSTRACT

In this study, the hydration behavior of gypsum paste mixed with bagasse and kenaf fibers as lignocellulosic material and fiberglass as inorganic material is evaluated. Moreover, the properties of gypsum-bonded fiberboard (GBFB) are examined using bagasse fibers (*Saccharum officinarum*·L), kenaf fibers (*Hibiscus cannabinus*·L) and industrial fiberglass. The weight ratios of fiberglass (at three levels 0, 3 and 6%), bagasse fiber (at three levels 0, 7.5 and 15%) and kenaf fiber (at three levels 0, 7.5 and 15%) to gypsum are used to make the gypsum-bonded fiberboard with the nominal density  $1.10 \text{ g}\cdot\text{cm}^{-3}$ . After preparing the fiberboard, its flexural properties were examined. Response surface methodology (RSM) and artificial neural network (ANN) were used to model the bending strength of gypsum-bonded fiberboard. According to the hydration tests, it was determined that as the extractives in the lignocellulosic materials increased, the temperature of the mixture decreased and its setting time increased. According to the bending test results, it was determined that there is an ideal consistency between the predicted values and the observed data, so that as bagasse and kenaf fiber increased, the modulus of rupture (MOR) increased. Maximum MOR of panel was predicted to be 10.81 MPa and 11 MPa by RSM and ANN at optimum condition. Based on the statistical analysis, the training and validation data sets of the studied models were compared by the coefficient of determination ( $R^2$ ), root mean squares error (RMSE) and mean absolute error (MAE). ANN model showed a much more accurate prediction than RSM in terms of the values  $R^2$ , RMSE and MAE.

#### Keywords:

Gypsum-bonded fiberboard  
RSM  
ANN  
Hydration  
MOR  
Bagasse  
Kenaf  
Glass fiber

#### Historic:

Received 03/12/2017  
Accepted 26/02/2018

#### <sup>†</sup>Correspondence:

morteza17172000@yahoo.com

#### DOI:

10.1590/01047760201824012484

<sup>1</sup> Shahid Beheshti University, University of Zabol, Tehran, Iran

<sup>2</sup> University of Zabol, Iran

<sup>3</sup> University of Zabol, Iran

<sup>4</sup> University of Zabol, Iran

<sup>5</sup> Shahid Beheshti University, Tehran, Iran

## INTRODUCTION

Panels with mineral binders have extensive applications in flooring, inner lining of walls, ceiling and partition walls. These panels, such as gypsum-bonded fiberboard, have a better linear stability than similar wood-based panels, and when exposed to fire, they show a higher resistance than other wood composite products. Adding cellulose fibers to a certain amount has a strengthening effect, and beyond the certain amount, they have negative effects. Moreover, the way the fibers are distributed in the mixture does not change the results. The comparison of the specimens containing fibers and the control specimens in a research by Rapoport et al. (2005) showed that the cracks observed due to the shrinkage from drying were narrower. For some time, organic fibers were added to gypsum, but artificial fibers were mainly used, such as fiberglass (Eve et al. 2002). Fiberglass increases the flexural load-bearing capacity of the composites (Lempfer et al. 1990). Fiberglass has a proper strength and stiffness, preserves its mechanical properties at high temperatures, has proper resistance to moisture and corrosion and is rather cheap. The relationship between adding natural fibers to gypsum matrix and the mechanical properties of the composites was evaluated (Coutts 1990, Hernández-Olivares et al. 1992).

According to the properties of any binder, gypsum and cement improvement must lead to a product with better mechanical properties and higher resistance to moisture. Analysis of the extractives in the organic compounds is very important and can delay the hydration of the mineral binders and hence, it can affect the internal bonding and mechanical properties of gypsum-wood particleboards (Ahn and Moslemi 1980, Simatuupang et al. 1989). In a research on the chemical relationship between wood and cement, Hachmi and Campbel (1990) studied the wood extractives and wood-cement setting. Accordingly, extractives are complex compounds that contain resin, fatty acids, terpenes, phenols, tannins and sugars. These elements are largely different in terms of their solubility and their contents are different in different species. The most important constraint for making fiberboard using mineral binders is the highly variable compatibility between wood and mineral binders.

Various factors can affect the compatibility, such as the solubility of the extractives into water or alkaline environment (Hofstrand et al. 1984, Semple et al. 2000, Hachmi and Moslemi 1989, Moslemi and Lim 1984). Species containing more than 7% of the extractives dissolved into hot water can be considered

as incompatible materials (Hachmi and Moslemi 1989). Compounds of the extractives can delay the hydration. For reducing the incompatibility, it is suggested that extractives are obtained from wood using hot water and chemical additives (Moslemi et al. 1983, Zhengtian and Moslemi 1985). Conductimetry studies showed that for delaying the gypsum set in the system, the extractives delay the overall reaction. A comparative study of the penetration of acetic acid and phenolic compounds showed that these factors are the main reason of the slow-down of gypsum set. Improvement of mineral binders (cement, gypsum and soil) has become the main issue of concern in recent decades. It is tried to replace mineral reinforcing factors (fiberglass or asbestos fibers) by organic fibers such as sisal and craft pulp, or cellulose fibers (Coutts 1983, Coutts et al. 1994).

Natural fibers slow down the gypsum set due to the presence water-soluble compounds (Dalmay et al. 2010). The lack of wood and forest in many countries, cheapness and abundance of lignocellulosic resources during the seasons of the year are some main reasons of using agricultural wastes. Replacement of agricultural wastes with wood can help the improvement of environmental conditions, because resources are used correctly. According to what was mentioned above, many researches are conducted on using agricultural wastes and artificial fibers. Their effects on panel properties will be different due to the different shape of bagasse, kenaf and glass fibers, different chemical compositions and their different morphological and anatomical properties.

As mentioned above, the results obtained from experimental studies showed that many variables significantly affect the bending strength, such as different fiber types and additives. Hence, optimal conditions of manufacturing must be found, which provide a balance between product properties and manufacturing cost. However, it is too costly and time-consuming to determine the influence of each parameter on the bending strength. Thus, most recent researches have been focused on prediction of properties of different composites by modeling tools rather than comprehensive experimental procedures. Artificial neural network (ANN) can give a chance to achieve the logical values of bending properties by doing some experimental treatments because of its capability to determinate complex and non-linear relationship in the data structure (Kalogirou 2001, Zhang et al. 1998). Due to the advantages mentioned, ANN methods are applied in several studies for predicting mechanical and physical properties in the wood-based composites field. Cook and Chiu (1997), Fernandez et al. (2008) and Watanabe

et al. (2015) used the ANN approach for modeling the internal bond strength of particleboard. Ozsahin (2013) developed an artificial neural network (ANN) model for predicting the effects of some production factors on physical properties of oriented strand board (OSB). Demirkir et al. (2013) employed the same approach for modeling the plywood bonding strength. In literature, the effects of various factors on the mechanical and physical properties of wood-based composites are discussed mostly in detail, and ANN methods are used to predict the properties of these composites. However, it is shown that no information is available to investigate and predict the effects of fibers obtained from different resources on the bending strength of gypsum-bonded fiberboard. Hence in the present study, we aimed to investigate and predict the bending strength of gypsum-bonded fiberboard manufactured from different fibrous resources with a proper weight ratio of bagasse, kenaf and glass fiber to gypsum, and determine the best composition for producing gypsum-bonded fiberboard.

## MATERIAL AND METHODS

### Origin of data

Bagasse (*Saccharum Ossaicinarum* L.) was prepared from the southwest regions of Iran. Some worn-out kenaf sacks (*Hibiscus cannabinus* L.) were prepared also from a warehouse in Zabol. Fiberglass rolls were also prepared and transferred to the laboratory. The mineral binder was Omid-e-Semnan gypsum. The coarse particles of gypsum were first removed by a Mesh 40 Sieve, and fine particles were prepared to make the samples.

### Chemical analysis

For chemical analysis of lignocellulosic materials, lignin content, extractives soluble in alcohol-benzene solution and ash and silica of the raw kenaf and bagasse fibers were determined according to TAPPI T 222 om-98 (1998), TAPPI T 204 cm-97 (2004) and TAPPI T 211 om-85 (2009) standards, respectively. Ten specimens were used for each test. The results are shown in Table I.

### Hydration test and compressive strength

The hydration test was performed on the gypsum paste sample using calorimetric method to evaluate the compatibility of the materials used with gypsum by determining the temperature emitted when gypsum was mixed with or without kenaf, bagasse or glass fibers and water containing extractives. The paste's setting time is

**TABLE I** Analysis of fibers, from the species teste d.

Species	Cellulose (%)	Lignin (%)	Ash (%)	Extractives (%)	Silica (%)	Silica in ash (%)	Slenderness ratio
Bagasse	47.6	23.	1.7	4.1	0.9	42.9	68.8
Kenaf	57.1	12.	5.5	2.9	-	-	150.9
Fiberglass	-	-	-	-	-	-	≥ 300

a good index of the hydration reaction rate. Vicat test was performed to determine the consistency progress of the gypsum paste by recording the initial and final setting times during the change of the penetration depth of the needle of the Vicat apparatus over time. For this purpose, different weight ratios were used including 300g gypsum, 150 ml water and 15 g powder of lignocellulosic material for the treatments c, f and i, respectively, and 300 g gypsum, 150 ml pure water or extractives for the treatments g, a, b, d, e, h, j and k, respectively. For specimens with or without powder of fibers, the initial and final setting times were recorded that are a reliable parameter for determining the hydration speed. From the treatments mentioned above, specimens were also prepared in 20×20×30 mm mould for performing the compressive strength test.

### Panel preparation

The effect of independent variables was examined on the modulus of rupture of the boards prepared, including fiberglass at three levels 0, 3 and 6%, bagasse fibers at three levels 0, 7.5 and 15% and kenaf fibers at three levels 0, 7.5 and 15%. Other preparation factors were constant such as the amount of water (40% of dry weight of gypsum), board's density (1.10 g·cm<sup>-3</sup>), press closing speed (4.5 mm·s<sup>-1</sup>), press pressure (15 Kg·cm<sup>-2</sup>), press temperature (25 °C), press time (24h), board's thickness (10mm) and etc. The preparation process was a semi-dry process. First, water containing citric acid (99.95% water+ 100% citric acid 0.05) was sprayed on the dry fibers. After moistening the fibers in a laboratory mixer for 5 minutes, gypsum was sprinkled on them and they were remixed in a high speed mixer until a smooth homogeneous mixture of gypsum-fibers was obtained. The mixture was then put into a 30×30 cm wooden mold to prevent from changes in the cake's thickness and density in the final board. The cake was then put under the cold press. The boards were maintained by a clamp for 24 h at a constant pressure. After removing the clamps, the prepared boards were put into plastic bags for 48 h in order to complete the hydration process. Then, after removing the boards from plastic bags, they were exposed to the open air for 5 days in order that the moisture is balanced. After the boards were hardened,

their moisture ranged from 16 to 20%. So they had to be dried to achieve the desirable strength. For this purpose, the boards were dried into an oven at the temperature 50°C for 4 h under permanent ventilation. The boards were dried until the moisture 5 to 7% was reached. The final boards had the dimensions 1×35×35 cm. After drying, cutting and preparing the test specimens, modulus of rupture (MOR) was computed according to EN 319 Standard (1999). MOR was determined by HOUNS Field H25ks Mechanical Testing Machine.

### Experimental design

#### Response surface methodology

After performing bending strength test, the results were analyzed as the response surface using experimental data that presented mathematical relations based on the quadratic regression model. This technique was used for developing a mathematical model as multivariate regression equations for the properties of the boards made. Using the response surface methodology, the independent variables were considered as functions of a mathematical model. The mathematical model is denoted by a general quadratic (regression) Equation 1 for the response surface  $y$  (Balasubramanian et al. 2008), where  $x_i$  and  $x_j$  are input or independent factors,  $\beta_0$  is the free term of the equation, the coefficients  $\beta_1, \beta_2, \beta_i$  are linear terms;  $\beta_{11}, \beta_{22}, \beta_{ii}$  are quadratic terms;  $\beta_{12}, \beta_{13}, \beta_{i-1,j}$  are the interaction terms and the  $\epsilon$  represents the random error.

$$y = \beta_0 + \sum_{i=1}^k \beta_i x_i + \sum_{i < j} \sum_{i=1}^k \beta_{ij} x_i x_j + \sum_{i=1}^k \beta_{ii} x_i^2 + \epsilon \quad [1]$$

All coefficients of the cube's central axis were obtained using Expert Design software package. After determining the significance of the coefficients (at the level of confidence 95%), the final model was described only using the coefficients (Lakshminarayanan and Balasubramanian 2009). It is recommended that the six-center test is used for three variables (William and Cochran 1992). Hence, based on the equation 2 where  $n$  is the number of variables and  $k$  is the number of repetitions at the cube's center, the total number of tests required for three independent

$$2^n + (n \times 2) + k \quad [2]$$

$$2^3 + (3 \times 2) + 6 = 20 \quad [3]$$

variables (percentage of bagasse fibers, kenaf fibers and fiberglass) is [3]. When the regression analysis was performed, the response errors were obtained. The number of the independent variables, their codes and levels and the experimental design used are presented in Tables 2 and 4.

**TABLE 2** A Coded and actual levels of variables.

Species	Cellulose (%)	Lignin (%)	Ash (%)	Extractives (%)	Silica (%)	Silica in ash (%)	Slenderness ratio
Bagasse	47.6	23.	1.7	4.1	0.9	42.9	68.8
Kenaf	57.1	12.	5.5	2.9	-	-	150.9
Fiberglass	-	-	-	-	-	-	≥ 300

#### Artificial neural network

ANNs are more powerful techniques in predicting non-linear relationships than the RSM technique, because they require many more experiments than the RSM. However, while the statistical relationships between input and output districts were significant according to the design of experiments (obtained by RSM), ANN methods can also work correctly even with logical small data (Shanmugaprakash and Sivakumar 2013). Therefore, the experimental data achieved by RSM could be adequate to organize ANN model effectively. A multilayer perceptron (MLP) was selected as a feed-forward ANN consisting of three main layers called the input (operated using the hyperbolic tangent sigmoid transfer function), hidden and output layers (operated using the pure-linear transfer function) (Mirsoleimani-Azizi et al. 2015, Movagharnejad and Nikzad 2007) as described by Equation (4).

$$f(x) = \text{tansig}(x) = \frac{1 - e^{-x}}{1 + e^{-x}} \quad [4]$$

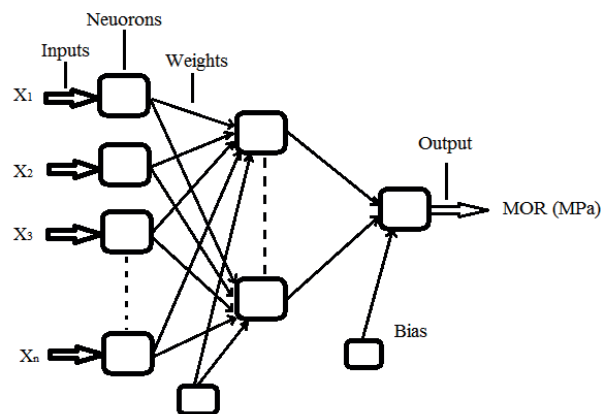


**FIGURE 1** The ANN architecture used as the prediction model for MOR.

A MLP was developed in MATLAB (The Mathworks, Inc., R2014a) with three input neurons representing the glass fiber, kenaf fiber and bagasse fiber content, a single hidden layer of neurons, and one output neurons representing the MOR of gypsum-bonded fiberboard. As seen from MLP architecture (Figure 1), the number of neurons required in the hidden layer is determined by adding the weighted inputs and the related bias (Equation 5) and also leading the input data towards a more nonlinear situation; so at least 8 neurons were needed to fix the final model using the data obtained to develop the RSM, and the addition of more neurons made the model overfitting possible (Cheok et al. 2012, Madadlou et al. 2009).

$$x_j = \sum_{i=1}^p y_i w_{ji}^{in} + b_j^{in} \quad [5]$$

To obtain the final model, all experimental data sets were divided evenly into three subsets: 70% of data sets (14 samples) were used for training the network, 15% (3 samples) were used for validation and the last 15% (3 samples) were used for testing sets. The number of neurons in the input layer is determined by the number of inputs, and those in the output layer are determined by the number of outputs (Wang and Wan 2009). The number of neurons in the hidden layer is determined by repetition in testing a number of neural networks until the mean square error (MSE) value of the output reaches a minimum.

## RESULTS AND DISCUSSION

### Hydration Test

The effect of the type of lignocellulosic material and the water-soluble extractives of these materials was evaluated on hydration process of gypsum paste by measuring the final setting time ( $t_{max}$ ) and maximum hydration temperature ( $T_{max}$ ) of the gypsum+ lignocellulosic material (bagasse and kenaf) mixture or gypsum+ extractives (from washing the lignocellulosic material with hot and cold water) mixture.  $T_{max}$  and  $t_{max}$  values of the test samples are given in Table 3.

**TABLE 3** Hydration temperature and time to reach the maximum temperature.

Treatment cod	Treatment	Treatment type	Maximum temperature (°C)	Curing time (min)
60	52	gypsum+ water	A	G.W
205	46	gypsum+ citric acid 0.05	B	G. A 0.05
285	40	gypsum+ citric acid 0.05+bagasse	C	G. A 0.05. B
305	41	gypsum+ citric acid 0.05+bagasse cold-water extractives	d	G. A 0.05 BCE
340	38	gypsum+ citric acid 0.05+bagasse hot water extractives	e	G. A 0.05 BHE
195	41	gypsum+ citric acid 0.05+kenaf	f	G. A 0.05. K
235	42	gypsum+ citric acid 0.05+kenaf cold water extractives	g	G. A 0.05 KCE
280	39	gypsum+ citric acid 0.05+kenaf hot water extractives	h	G. A 0.05 KHE
185	44	gypsum+ citric acid 0.05+fiber glass	i	G. A 0.05. G
178	44	gypsum+ citric acid 0.05+fiber glass cold water extractives	j	G. A 0.05 GCE
180	43	gypsum+ citric acid 0.05+fiber glass hot water extractives	k	G. A 0.05 GHE

Note: Different weight ratios included 300g gypsum, 150 ml water and 15 g lignocellulosic material for the treatments c, f and i, and 300 g gypsum, 150 ml water for the treatments a, b, d, e, g, h, j and k.

The results showed that the final setting time of the gypsum increased at the maximum temperature at the presence of the lignocellulosic material or extractives from washing the lignocellulosic material (Figure 2), and then, the maximum temperature of the mixture decreased. In addition, the increase or decrease of the hydration at different times depends on the type of the lignocellulosic material and the extractives content. Generally, kenaf with less extractives (Table 3) has a higher maximum hydration temperature and lower hydration time.

According to Zhou and Kamdem (2002), the decrease in maximum temperature may be due to the presence of the hygroscopic sponge tissue in pith or extractives in lignocellulosic materials that prevents from heat generation due to water absorption. The results indicate that as raw lignocellulosic material or water-soluble extractives obtained from washing lignocellulosic material are added, the hydration temperature decreases and the final setting time increases. In Figure 2, among the test treatments with two types of lignocellulosic materials (bagasse and kenaf) and along with treatments with extractives from washing with hot and cold water, maximum hydration temperature was related to the treatment of gypsum+citric acid 0.05 with kenaf fiber extractives washed with cold water, showing the temperature 42 °C and the final setting time 235 min. Since the extractives in bagasse are 1.5 times more

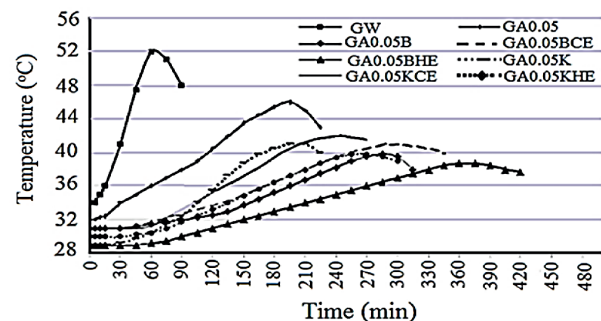


**FIGURE 2** Hydration temperature and time of the test samples (fiberglass was excluded).

than those in kenaf (Table 1), and washing with hot water contains more extractives, minimum hydration temperature was for the treatment of gypsum+citric acid 0.05 with bagasse fiber extractives washed with hot water, showing the temperature 38 °C and the longest final setting time 340 min.

Analysis of the results in Tables 1, 3 and Figure 2 shows that washing the lignocellulosic material with hot water results in the solution of more extractives that changes the hydration temperature and setting time of gypsum paste.

During the gypsum hydration process, like calcium hydroxide, calcium sulfate increases the pH of the gypsum paste when adding water to the hydration process. On the other hand, the extractives of plant fibers are generally acidic and they delay the minerals set due to the presence of sugar and extractives. Therefore, the system pH will change that may change the speed of the hydrated compounds formation; Hence, the hydration process can be negatively affected. Alkaline hydrolysis of hemicellulose and lignin is due to the formation of lignin calcium salts, polysaccharide and decrease of some sugar substances (Singh 1979). These soluble salts or deposits interfere with the hydration of the mineral physically and chemically and even can change the composition and morphology of the hydrated product (Roberts, 1967). In addition, sugar substances of wood are active hydrophilic materials. Besides setting, sugar substances added to water in the mixture of gypsum mineral create a thin layer of densified water on the surface of gypsum grains as impenetrable gel under the effect of absorbency and coherence of the molecule. Although tiny gypsum particles are not compact, they are out of access of water. Therefore, the progress of hydration process is impossible and its speed slows down (Vaickelionis and Vaickelionis 2006).

### Vicat

The effect of the type of lignocellulosic material and extractives on the setting time of gypsum paste during the vicat test is shown in figure 3. The setting time of the gypsum paste was 40 min without any additive. Acid solvent (citric acid 0.05%) was used to delay the setting speed of the gypsum paste, and the setting time increased to 165 min. Among the test treatments, the lowest setting time was for the mixture of pure gypsum and water followed by the treatment f (gypsum+ citric acid 0.05+kenaf), i.e. 85 min. The reason can be the high volume of fibers, higher contents of cellulose and lower extractives in the lignocellulosic material (kenaf). In other words, the lower the extractives of the lignocellulosic material in gypsum paste, the shorter the setting time of the paste.

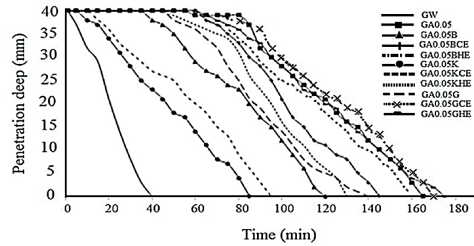


FIGURE 3 Vicat test: penetration depth needle into of the gypsum pastes.

In addition, the paste of the mixture of gypsum and bagasse fibers has led to water absorption by cell walls due to the low density and bagasse sponge structure. The increase in water absorption increases the concentration of gypsum paste, so that the penetration of vicat needle into the mixture is prevented while gypsum hydration has not completed yet. In fact, bagasse, kenaf and glass fibers act as filler and are the main factor of the decrease in the setting time. The higher content of extractives soluble in the gypsum paste resulting from washing bagasse with hot water can be also an effective factor and delays the gypsum's setting time.

### Compressive strength

The results from the compressive strength test are shown in Figure 4. The strengths range from 1 to 7 MPa. The compressive strength of the pure gypsum with water was highest in certain times (3, 8, 24 and 72 h).

The results showed that increasing the time, the compressive strength of the samples increases. The highest strengths were in 72 hours and the highest strength was for the pure gypsum sample (6.5 MPa). Adding citric acid 0.05% as the retarder of dehydration, the compressive strength decreases. The compressive strength of the pure gypsum + water containing citric acid 0.05% decreased to 5.1 MPa after 72 h. This can be due to the delay of the dehydration process and prevents from the formation of gypsum crystal lattice (Sanda 1982). Samples containing extractives have lower strength. The

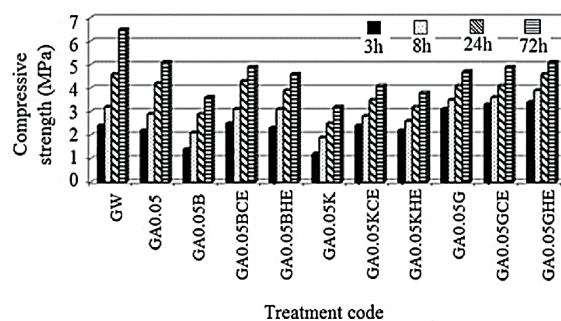


FIGURE 4 Compression strength of gypsum paste samples.

extractives delay the gypsum dehydration process and this can prevent from completion of hydration process and decreases the final strength of the cured mixture. On the other hand, for a constant wood to gypsum ratio, when the retarder of gypsum paste hydration is used, the compressive strength decreases. Generally, the lowest strength is for gypsum + bagasse or/and kenaf fibers samples. Values show that when lignocellulosic fibers are used in the test mixture, there is a lower strength than treatments in which only extractives are applied.

RSM model

The effect of the variables including fiberglass ( $X_1$ ), kenaf fiber ( $X_2$ ) and bagasse fiber ( $X_3$ ) on MOR predicted by the RSM model was compared to the experimental data, and the results can be observed in Table 4. The results are plotted in Figure 5 to provide the coefficient of determination ( $R^2 = 0.9070$ ).

Coefficients of each variable in the quadratic model and its estimated multiple regression equation are presented in Table 5 and Equation 5.

According to the regression coefficient (Table 5), it is observed that the linear coefficients ( $\alpha_1, \alpha_2, \alpha_3$ ) of MOR are positive. Positive values show that the increase in fiberglass, bagasse and kenaf fibers for making panels increases MOR. Maximum MOR is 11 MPa for the board N° 16 (6% fiberglass, 15% bagasse fibers and 15% kenaf fibers), meeting the standard

TABLE 4 The experimentally obtained MOR of panels compared to that predicted by RSM model and ANN.

Run	Actual values of variables (%)			Experimental MOR (MPa)	RSM predicted MOR (MPa) & Error	ANN predicted MOR (MPa) & Error
	X1	X2	X3			
1	0	15	15	6.70	7.02 (-0.32)	6.69 (0.0009)
2	3	7.5	7.5	6.30	6.34 (-0.04)	6.175 (0.125)
3	3	15	7.5	8.10	7.87 (0.23)	8.1 (-0.0003)
4	3	7.5	7.5	6	6.34 (-0.34)	6.175 (-0.175)
5	6	15	0	9.3	9.63 (-0.32)	9.943 (-0.643)
6	0	0	0	1.9	2.02 (-0.12)	1.9 (-0.000009)
7	0	15	0	5.9	5.83 (0.065)	5.49 (0.407)
8	3	7.5	7.5	6.5	6.34 (0.16)	6.175 (0.325)
9	3	7.5	7.5	6.3	6.34 (-0.04)	6.175 (0.125)
10	6	0	15	8.9	8.49 (-0.41)	8.902 (-0.0026)
11	3	0	7.5	5	4.81 (0.19)	4.99 (0.00064)
12	3	7.5	15	7.4	7.53 (-0.13)	7.4 (-0.0008)
13	3	7.5	0	5.3	5.15 (0.15)	5.3 (-0.0016)
14	6	7.5	7.5	8.70	8.46 (0.24)	8.7 (0.000008)
15	0	7.5	7.5	5.6	5.12 (0.48)	6.1 (0.699)
16	6	15	15	11	10.81 (0.2)	11.00 (-0.0002)
17	3	7.5	7.5	6.4	6.34 (0.06)	6.175 (0.225)
18	6	0	0	4.8	4.91 (-0.11)	4.79 (0.007)
19	3	7.5	7.5	6.00	6.34 (-0.34)	6.175 (-0.175)
20	0	0	15	5.5	5.6 (-0.1)	4.96 (-0.53)

( $X_1$ ), kenaf fiber ( $X_2$ ) and bagasse fiber ( $X_3$ )

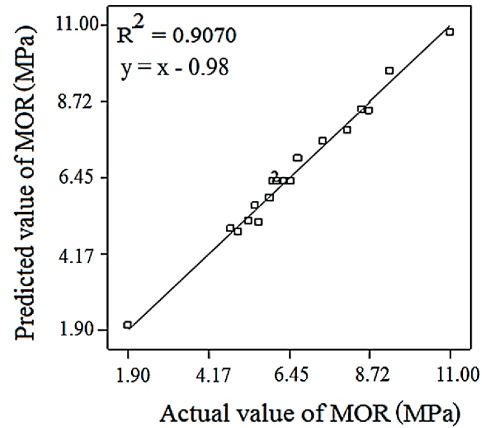


FIGURE 5 Compression strength of gypsum paste samples.

Bison (Hz) (1978) and EN 634-2 (2007), that is 9 MPa. It is clear from Table 5 that the quadratic terms (glass fiber ( $X_1^2$ )), interactive term (glass fiber  $\times$  kenaf fiber ( $X_1X_2$ ) and kenaf fiber  $\times$  bagasse fiber ( $X_2X_3$ )) and linear terms (glass fiber ( $X_1$ ), kenaf fiber ( $X_2$ ) and bagasse fiber ( $X_3$ )) have large effects on the MOR due to their higher F values as well as lower p-values.

ANOVA was used to illustrate which variables are statistically significant in the determination of MOR at the confidence interval 95% (Table 6). MOR values range from 1.9 to 11 MPa. According to Table 6, the Model F-value of 166.27 shows the model is significant. In fact, there is no chance that a "Model F-Value" is equal to this value due to the noise. Values less than 0.0500 for  $X_1$ ,  $X_2$ ,  $X_3$ ,  $X_1X_2$ ,  $X_2X_3$ ,  $X_1^2$  indicate that these model terms are significant, namely model reduction may improve the model (Table 5). The value 2.65% for the "Lack of Fit F-value" shows that the Lack of Fit is not significant relative to the pure error which it is good. Moreover, a high F value (166.27) with a low probability ( $p=0.0001$ ) indicates the high ability of the model in predicting the results. The predicted R-squared of 0.9070 is in full agreement with the adjusted R-squared of 0.8812.

TABLE 5 Regression analysis of RSM model for the MOR of panels, with the associated statistical significance of each coefficient.

Coefficient	Value	F-value	p-value
$\beta_0$	6.39	123.45	< 0.0001
$\beta_{x1}$	1.67	442.43	< 0.0001
$\beta_{x2}$	1.53	371.36	< 0.0001
$\beta_{x3}$	1.19	224.65	< 0.0001
$\beta_{x1x1}$	0.59	15.00	0.0031
$\beta_{x2x2}$	-0.014	0.00811	0.9300
$\beta_{x3x3}$	-0.21	1.99	0.1886
$\beta_{x1x2}$	0.22	6.42	0.0296
$\beta_{x1x3}$	0.13	1.98	0.1894

**TABLE 6** Analysis of variance (ANOVA).

Source	Sum of squares	df	F-value	P-value
Model	69.76	6	166.27	0.0001
Residual error	0.63	10	-	-
Lack-of-fit	0.74	8	2.65	0.1487
Pure error	0.17	5	-	-
R-Squared = 0.9070		Adj R-Squared = 0.8812		

The direct effect of three variables on the MOR is shown in figure 6. When the content of glass fiber, kenaf fiber and bagasse fiber in the panel varied from 0 to 6%, 0 to 15% and 0 to 15%, respectively, MOR value increased continuously, but the effect of glass fiber content is greater than others as shown in figure 6 and Table 5.

The interactive effects of the variables (bagasse × kenaf fibers content and kenaf fibers × glass fiber) showed that increasing the content of glass, kenaf and bagasse fibers, the flexural strength (MOR) also increases (Figure 7).

The reason can be attributed to the high flexibility and slenderness ratio of the fibers (Mashima et al. 1994, Takahashi 1986). This fact affects the brittleness of gypsum composites. Due to their high slenderness ratio, mineral fibers such as fiberglass also improve the flexural strength and stiffness of the panels based on mineral binders such as gypsum. This result was in agreement with the previous study that using natural fibers such as bagasse combined with other lignocellulosic waste materials for making gypsum-bonded particleboard increases the flexural strength due to their desirable flexibility (Nazerian and Kamyab 2013). The lowest value of MOR is related to the specimen without any fiber (Figure 7). According to Table 1, the slenderness ratio of fiberglass, bagasse and kenaf fibers is ≥ 300, 68.8 and

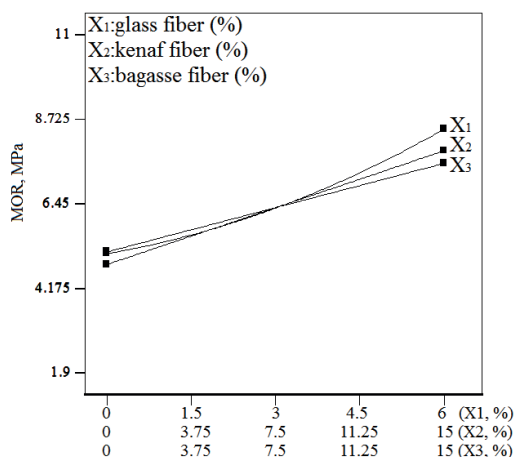


**FIGURE 6** Direct effect of the glass, kenaf and bagasse fiber contents on MOR.

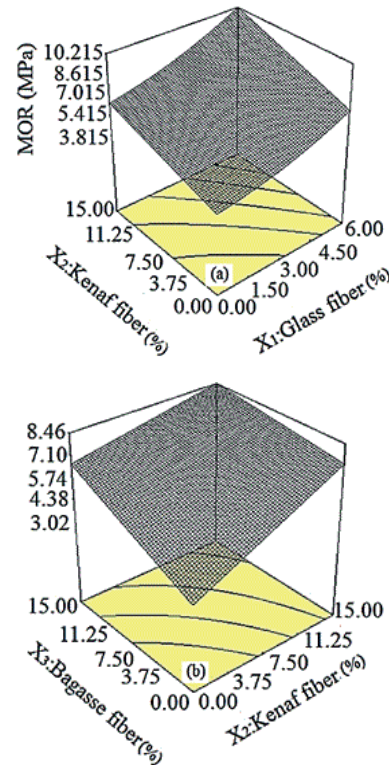


**FIGURE 7** Direct effect of the glass, kenaf and bagasse fiber contents on MOR.

150.9, respectively, showing that the slenderness ratio of fiberglass is much higher than that of bagasse and kenaf fibers. It is observed that the higher the fiberglass used for making gypsum-bonded fiberboard compared to bagasse and kenaf fibers, the flexural strength properties (MOR) increase (Figure 7). The reason can be attributed to the strong effective grid produced due to the connections between gypsum particles and fiberglass surface. These fibers are largely compatible with minerals and lead to a rather strong connection and mix with minerals desirably (Eusebio and Suzuki 1990, Bogue 1964, Hachmi and Moslemi 1990). Fiberglass is resistant to alkalis and significantly affects the composite quality due to its surface activities and hence, it has desirable compatibility with mineral (Eusebio and Suzuki 1990). Due to their high desire to form a bond with minerals, mineral fibers provide better and stronger bonding conditions for the cohesion between wood, fibers and cement (Mashima et al. 1994, Eusebio and Suzuki 1990). Findings of Cao et al. (2006) and Ganesan et al. (2007) showed that using fibers for making fiber-cement composites improved the mechanical properties, especially the flexural strength. They attributed the reason to the high contact surface, formation of a more effective grid and increase in the cohesion of fibers with cement particles.

Artificial neural network

In order to determine the suitability of the model, the experimental (actual) values of MOR were compared to those predicted by ANN model. The experimental and predicted values for each experiment were plotted against the run numbers (Figure 8). This figure consists of the perfect fit line  $y=x$  (predicted data = experimental data with a high degree of correlation) and best fit line described by the best linear equation ( $y = mx + c$ ) with a high coefficient of determination ( $R^2 = 0.9837$ ).

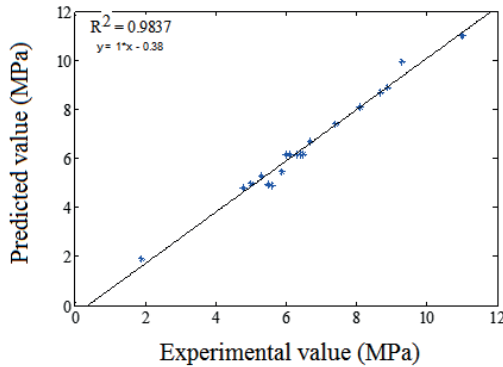


FIGURE 8 Correlation coefficient for mean MOR (ANN).

In order to predict the MOR values of gypsum-bonded fiberboard, the experimental data were grouped into four data sets. The number of hidden neurons between 4 and 10 was selected and evaluated to determine a favorable ANN model. Mean square error (MSE) of the selected hidden neurons in the model was calculated, including 4, 6, 8 and 10 (0.6, 0.065, 0.007 and 0.35, respectively). Hence, 8 hidden neurons were chosen for the model.

The results of MOR value prediction using the developed ANN model are exhibited in Table 4, which included an input layer with three neurons (content of glass fiber, kenaf fiber and bagasse fiber), an output layer with one neuron (MOR value), and 8 hidden neurons. According to the data sets used in the ANN prediction model (Figure 9), the correlation coefficient (R) of the predicted values (output) versus the actual values (target) were 0.99946, 0.98783, 0.99942 and 0.99183 for the training, validation, testing and all data sets, respectively.

These R values between experimental response and ANN predicted response showed in all the cases that there was a good correlation between the experimental and predicted values; so the developed ANN model trained using experimental data predicted the studied response (MOR) of panels precisely.

These R values between experimental and predicted values showed in all the cases that there was a good correlation between the actual and predicted values;

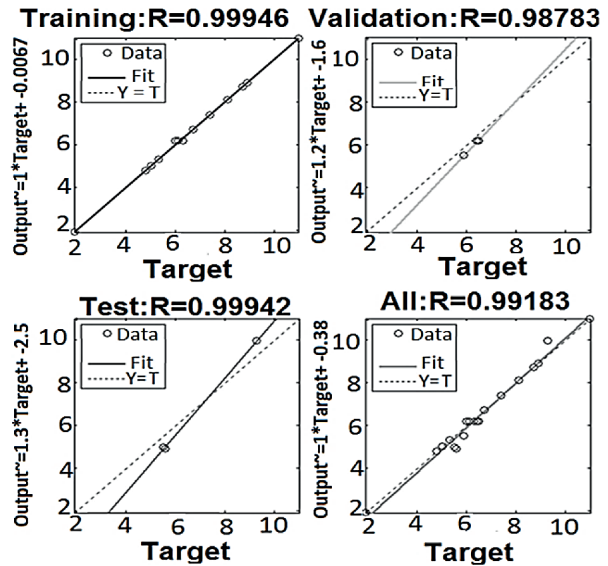


FIGURE 9 Correlation coefficient for mean MOR (ANN).

and the developed ANN model, which was trained using actual values, predicted the panel MOR precisely. Also,  $R^2$  value suggests that 99.88% of the variation in the actual and predicted values can be explained by the model.

Comparison of RSM and ANN

In order to estimate accurate prediction of the developed models, actual mean MOR values were compared with the mean MOR predicted values of the ANN and RSM models as shown in figure 10. It is observed in the figure that the prediction of mean MOR in both models is in full agreement with that of actual values; so the experimental values are approximated by trained neural network efficiently. However, RSM model was slightly accurate.

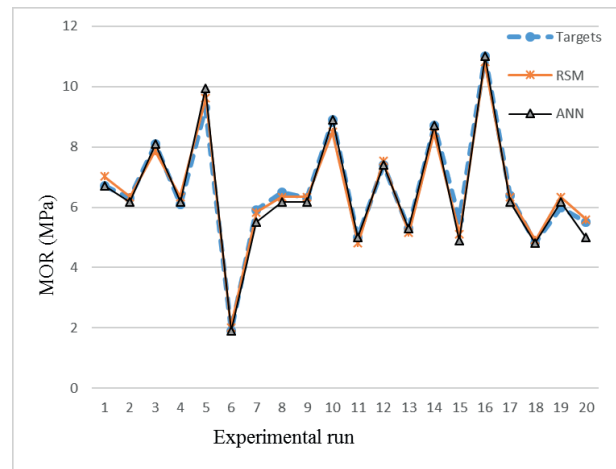


FIGURE 10 Comparison of RSM and ANN predictions with the experimental mean values of MOR.

ANN model predictions fit the line of perfect prediction more than RSM model. Thus, ANN model is more capable of data generalization than RSM model. This higher accuracy of prediction by ANN can be related to its approximation ability through nonlinearity of the system (Maran et al.2013), whereas RSM belongs only to a second-order polynomial (Shanmugaprakash and Sivakumar 2013). However, the negative effect of using ANN technique lies in its limited prediction due to the application of some studied variables and factors through the training process (Rajkovic et al. 2013).

**TABLE 7** Performance evaluation of RSM and ANN models.

Coefficient	Value	F-value	p-value
$\beta_0$	6.39	123.45	< 0.0001
$\beta_{x1}$	1.67	442.43	< 0.0001
$\beta_{x2}$	1.53	371.36	< 0.0001
$\beta_{x3}$	1.19	224.65	< 0.0001
$\beta_{x1x1}$	0.59	15.00	0.0031
$\beta_{x2x2}$	-0.014	0.00811	0.9300
$\beta_{x3x3}$	-0.21	1.99	0.1886
$\beta_{x1x2}$	0.22	6.42	0.0296
$\beta_{x1x3}$	0.13	1.98	0.1894

ANN predicted values of the experimental samples of MOR and their errors are given in Table 4. The model showed good prediction performance. Moreover, the results indicated that the values predicted by ANN had a low percent of error that is satisfactory for predicting MOR values.

$R^2$ , Adjusted  $R^2$ , RMSE and MAE values used to evaluate the performance of ANN and quadric models developed in this study are given in Table 7. The calculated  $R^2$  and adjusted  $R^2$  of the ANN model were 0.9837 and 0.9619, respectively; however, the determination coefficients and adjusted determination coefficients for RSM models were 0.9070 and 0.8812, respectively.

The high value of  $R^2$  obtained for ANN model is indicative of its better fit (Joglekar and May 1987). The model's generalizability can be verified by its prediction accuracy for a validation data set (Eslah et al. 2012). RMSE and MAE values for ANN were less than those for RSM as shown in Table 1. These results show that the predication of RSM model has a greater deviation than the prediction of ANN model. This also means that the experimental data are fitted with a higher accuracy using the ANN model.

As seen from the results, ANN approach has shown better prediction performance than the quadratic approach based on the evaluation criteria and has a sufficient accuracy level in the prediction of MOR values. The determination coefficient ( $R^2$ ) between the measured and predicted values is used to check the adequacy of

the models. The relationships between these values obtained using the CCRD and ANN models are shown in figures 5 and 8, respectively. According to Figure 8,  $R^2$  values in training, validating and testing the data sets for MOR are greater than 0.99%. This result implies that the model designed is capable of explaining at least 0.99% of the measured data. These values also support the applicability of ANN. On the other hand,  $R^2$  values in quadratic model are 90.70% for MOR, which are desirable. These results indicated that the models used in both methods can be selected for accurate predictions, since they both have high explanatory values. However, the normal probability diagram of the measured-predicted values for ANN and quadratic models show that in the ANN model, data are more closely distributed on straight line (Figure 8) than those in quadratic model (Figure 5). This means that the errors in ANN model are distributed more normally. Hence, ANN model is selected as the regression model of MOR. Other studies are carried out about the strength properties of wood-based composites, but  $R^2$  values obtained by ANN and quadratic models in this study are higher compared to other studies (FERNANDEZ et al. 2008, DEMIRKIR et al. 2013, ESLAH et al. 2012).

The interactions among three parameters investigated for the bending strength of the panels are examined using three dimensional surface plots (Figure 11).

As it can be seen, there is a considerable similarity between Figures 7 and 11. The relationship between the content of kenaf fiber and glass depicted in Figure 7. The figure shows both parameters interact with each other, which significantly affects the MOR value of the panels. MOR value of the panels is highest at the highest kenaf and glass fiber loading. As the loading of both kenaf and glass fibers decreases, MOR value of the panels decreases.

MOR value decreased from over 10.11 MPa to less than 4MPa. Similarly, figure 11 shows MOR value as a function of input parameters including the content of kenaf fiber and bagasse fiber in three dimensional patterns. The lowest MOR value is observed at kenaf fiber content loading 0% and bagasse content 0%. Increasing the content of kenaf and bagasse fibers, MOR value of panels increases; so, MOR value decreased from over 8.9 MPa to less than 2.4MPa.

## CONCLUSION

The study of the hydration process showed that the higher the non-wood extractives, the higher the setting time of the paste containing the extractives. On the other hand, the resulting temperature decreases.

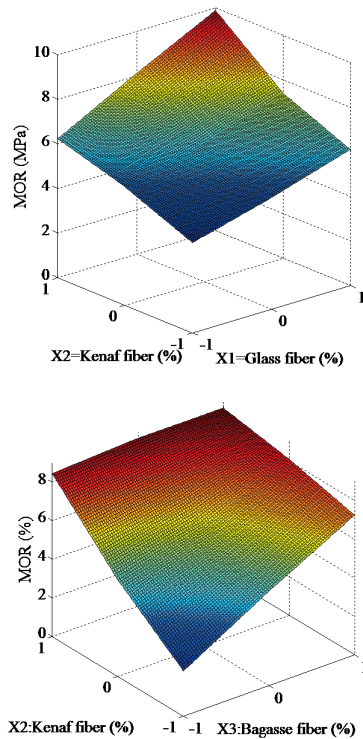


FIGURE 11 Three dimensional surface plots by ANN.

Moreover, the longest setting time of the test treatments is related to pure gypsum with water. In addition, among treatments in which only fibers are used in the gypsum paste, the longest setting time is related to the paste containing bagasse fibers.

Production of gypsum-bonded fiberboard using bagasse fibers, kenaf fibers and fiberglass as the reinforcing fibers increases the bending strength of the boards. Increasing bagasse and kenaf fibers when making mineral composites, the MOR increase, but the effect of fiber glass was higher than others.

The flexural properties modeling were developed to predict the bending strength. The prediction of not only ANN model but also RSM were found to be in good agreement with experimental data.

The predictive ANN model is found to be capable of better predictions of flexural properties within the range that they had been trained. The results of the ANN model indicate it is much more confident and accurate in estimating the values of bending strength when compared with the response surface model

## REFERENCES

AHN, W. Y.; MOSLEMI, A. SEM examination of wood-Portland cement bonds. **Wood Science**, v. 13, n. 2, p. 77-82, 1980.

AHN, W.Y.; MOSLEMI, A. SEM examination of wood-Portland cement bonds. **Wood Science**, v. 13, n. 2, p. 77-82, 1980.

B.W.-C. BOARD, Bison-Report, Links, 1978.

BALASUBRAMANIAN, M.; JAYABALAN, V.; BALASUBRAMANIAN, V. A mathematical model to predict impact toughness of pulsed-current gas tungsten arc-welded titanium alloy. **International Journal of Advanced Manufacturing Technology**, v. 35, n. p. 852-858, 2008.

BOGUE, R. H. The chemistry of Portland cement, Reinhold publishing corporation, USA, 1964.

CAO, Y., SHIBATA, S.; FUKUMOTO, I. Fabrication and flexural properties of bagasse fiber reinforced biodegradable composites. **Journal of Macromolecular Science**, v. 45, n. 4, p. 463-474, 2006.

CHEOK, C. Y.; CHIN, N. L.; YUSOF, Y. A.; TALIB, R. A.; LAW, C. L. Optimization of total phenolic content extracted from *Garcinia mangostana* Linn. hull using response surface methodology versus artificial neural network. **Industrial Crops and Products**, v. 40, n. ,p. 247-253, 2012.

COOK, D. F; CHIU, C. Predicting the internal bond strength of particleboard, utilizing a radial basis function neural network. **Engineering Applications of Artificial Intelligence**, v. 10, n. 2, p. 171-177, 1997.

COUTTS, R. Banana fibres as reinforcement for building products. **Journal of Materials Science Letters**, v. 9, n. 10, p. 1235-1236, 1990.

COUTTS, R. Flax fibres as a reinforcement in cement mortars. **International Journal of Cement Composites and Lightweight Concrete**, v. 5, n. 4, p. 257-262, 1983.

COUTTS, R. S. P. Banana fibres as reinforcement for building products. **Journal of Materials Science Letters**, v. 9, n. 10, p. 1235-1236, 1990.

COUTTS, R.; NI, Y.; TOBIAS, B. Air-cured bamboo pulp reinforced cement, **Journal of Materials Science Letters**, v. 13, n. 4, p. 283-285, 1994.

DALMAY, P.; SMITH, A.; CHOTARD, T.; SHAY-TURNER, P.; GLOAGUEN, V.; KRAUSZ, P. Properties of cellulosic fibre reinforced plaster: influence of hemp or flax fibres on the properties of set gypsum. **Journal of Material Science**, v. 45, n. 3, p. 793-803, 2010.

DEMIRKIR, C.; OZSAHIN, S.; AYDIN, I.; COLAKOGLU, G. Optimization of some panel manufacturing parameters for the best bonding strength of plywood. **International Journal of Adhesion and Adhesives**, v. 46, p. 14-20, 2013.

EN 634-2, Cement-bonded particleboards-Specifications-Part 2: Requirements for OPC bonded particleboards for use in dry, humid and external conditions, European Standardization Committee, Brussels, Belgium, 2007.

- ESLAH, F.; ENAYATI, A.; TAJVIDI, M.; FAEZIPOUR, M. Regression models for the prediction of poplar particleboard properties based on urea formaldehyde resin content and board density. **Journal of Agricultural Science and Technology**, v. 14, n. 6, p. 1321-1329, 2012.
- EUSEBIO, D.; SUZUKI, M. Production and properties of plant materials cement-bonded composites, Bulletin of the Experiment Forests, **Tokyo University of Agriculture and Technology**, v. 27, p. 27-38, 1990.
- EVE, S.; GOMINA, M.; GMOUH, A.; SAMDI, A.; MOUSSA, R.; ORANGE, G. Microstructural and mechanical behaviour of polyamide fibre-reinforced plaster composites. **Journal of the European Ceramic Society**, v. 22, n. 13, p. 2269-2275, 2002.
- FERNANDEZ, F. G.; ESTEBAN, L. G.; DE PALASIOS, P.; NAVARRO, M.; CONDE, M. Prediction of standard particleboard mechanical properties utilizing an artificial neural network and subsequent comparison with a multivariate regression model. **Forest Systems**, v. 17, n. 2, p. 178-187, 2008.
- GANESAN, K.; RAJAGOPAL, K. Thangavel, Evaluation of bagasse ash as supplementary cementitious material. **Cement and Concrete Composites**, v. 29, n. 6, p. 515-524, 2007.
- HACHMI, M. H.; MOSLEMI, A. Correlation between wood-cement compatibility and wood extractives. **Forest Products Journal**, v. 39, n. 6, p. 55-58, 1989.
- HACHMI, M. H.; MOSLEMI, A. Effect of wood pH and buffering capacity on wood-cement compatibility. **Holzforschung**, v. 44, n. 6, p. 425-430, 1990.
- HACHMI, M. N.; MOSLEMI, A. Correlation between wood-cement compatibility and wood extractives. **Forest Products Journal**, v. 39, n. 6, p. 55-58, 1989.
- HERNANDEZ-OLIVARES, F.; OTEIZA, I.; DE VILLANUEVA, L. Experimental analysis of toughness and modulus of rupture increase of sisal short fiber reinforced hemihydrated gypsum. **Composite Structures**, v. 22, n. 3, p. 123-137, 1992.
- HERNANDEZ-OLIVARES, F.; OTEIZA, I., DE VILLANUEVA, L. Experimental analysis of toughness and modulus of rupture increase of sisal short fiber reinforced hemihydrated gypsum. **Composite Structures**, v. 22, n. 3, p. 123-137, 1992.
- HOFSTRAND, A.; MOSLEMI, A.; GARCIA, J. F. Curing characteristics of wood particles from nine northern Rocky mountain species mixed with Portland cement. **Forest Products Journal**, v. 34, n. 2, p. 57-61, 1984.
- HOFSTRAND, A.; MOSLEMI, A.; GARCIA, J. F. Curing characteristics of wood particles from nine northern Rocky Mountain species mixed with Portland cement. **Forest Products Journal**, v. 34, n. 2, p. 57-61, 1984.
- JOGLEKAR, A.; MAY, A. Product excellence through design of experiments, **Cereal Foods World**, v. 32, p. 857-364, 1987.
- KALOGIROU, S. A. Artificial neural networks in renewable energy systems applications: a review. **Renewable and Sustainable Energy Reviews**, v. 5, n. 4, p. 373-401, 2001.
- LAKSKHMINARAYANAN, A.; BALASUBRAMANIAN, V. Comparison of RSM with ANN in predicting tensile strength of friction stir welded AA7039 aluminium alloy joints. **Transactions of Nonferrous Metals Society of China**, v. 19, n. ,p. 9-18, 2009.
- LEMPFER, K.; HILBERT, T.; GUNZERODT, H. Development of gypsum-bonded particleboard manufacture in Europe. **Forest Products Journal**, v. 40, n. 6, p. 37-40, 1990.
- LEMPFER, K.; HILBERT, T.; Gunzerodt, H. Development of gypsum-bonded particleboard manufacture in Europe. **Forest Products Journal**, v. 40, n. 6, p. 37-40, 1990.
- MADADLOU, A.; EMAM-DJOMEH, Z.; MOUSAVI, M. E.; EHSANI, M.; JAVANMARD, M.; SHEEHAN, D. Response surface optimization of an artificial neural network for predicting the size of re-assembled casein micelles. **Computers and Electronics in Agriculture**, v. 68, n. ,p. 216-221, 2009.
- MARAN, J. P.; SIVAKUMAR, V.; THIRUGNANASAMBANDHAM, K.; SRIDHAR, R. Artificial neural network and response surface methodology modeling in mass transfer parameters predictions during osmotic dehydration of Carica papaya L. **Alexandria Engineering Journal**, v. 52, n. 3, p. 507-516, 2013.
- MASHIMA, M.; KOUZA, K.; OHNO, S. Fiber reinforced cement and concrete (in Japanese), Gihoudou Press, Japan, 1994.
- MIRSOLEIMANI-AZIZI, S. M.; AMOOEY, A. A.; GHASEMI, S.; SALKHORDEH-PANBECHOULEH, S. Modeling the Removal of Endosulfan from Aqueous Solution by Electrocoagulation Process Using Artificial Neural Network (ANN), **Industrial & Engineering Chemistry Research**, v. 54, n. , p. 9844-9849, 2015.
- MOSLEMI, A. Fiber and Particleboards Bonded with Inorganic Binders: International Conference: Papers, Forest Products and Research Society, 1989.
- MOSLEMI, A. Fiber and Particleboards Bonded with Inorganic Binders: International Conference: Papers, Forest Products Research Society 1989.
- MOSLEMI, A.; GARCIA, J. F.; HOFSTRAND, A. Effect of various treatments and additives on wood-Portland cement-water systems. **Wood and Fiber Science**, v. 15, n. 2, p. 164-176, 1983.
- MOSLEMI, A.; LIM, Y. Compatibility of southern hardwoods with Portland cement. **Forest Products Journal**, v. 34, n. (7/8), p. 22-26, 1984.
- Movagharnejad, K.; Nikzad, M. Modeling of tomato drying using artificial neural network, **Computers and Electronics in Agriculture**, v. 59, n. , p. 78-85, 2007.

- NAZERIAN, M.; KAMYAB, M. Gypsum-bonded particleboard manufactured from agricultural based material. **Forest Science and Practice**, v. 15, n. 4, p. 325-331, 2013.
- OZSAHIN, S. Optimization of process parameters in oriented strand board manufacturing with artificial neural network analysis, **European Journal of Wood and Wood Products**, v. 71, n. 6, p. 769-777, 2013.
- RAJKOVIC, K. M.; AVRAMOVIĆ, J. M.; MILIĆ, P. S.; STAMENKOVIĆ, O. S.; VELJKOVIĆ, V. B. Optimization of ultrasound-assisted base-catalyzed methanolysis of sunflower oil using response surface and artificial neural network methodologies. **Chemical Engineering Journal**, v. 215-216, p. 82-8, 2013.
- RAPOPORT, J. R.; SAHAH, S. P. Cast-in-place cellulose fiber-reinforced cement paste, mortar, and concrete. **ACI Materials Journal**, v. 102, n. 5, p. 299-306, 2005.
- RAPOPORT, J. R.; SHAH, S. P. Cast-in-place cellulose fiber-reinforced cement paste, mortar, and concrete. **ACI Materials Journal**, v. 102, p. 299-306, 2005.
- ROBERTS, M. H. Effect of admixtures on the composition of the liquid phase and early hydration reactions in Portland cement pastes, International Symposium on Admixtures for Mortar and Concrete /Belg/, 1967.
- SANAD, M.; COMBE, E.; GRANT, A. The use of additives to improve the mechanical properties of gypsum products. **Journal of Dental Research**, v. 61, n. 6, p. 808-810, 1982.
- SEMPLE, K.; EVANS, P. D.; CUNNINGHAM, R. B. Compatibility of 8 temperate Australian Eucalyptus species with Portland cement. **European Journal of Wood and Wood Products**, v. 58, n. 5, p. 315-316, 2000.
- SHAMUGAPRAKASH, M.; SIVAKUMAR, V. Development of experimental design approach and ANN-based models for determination of Cr (VI) ions uptake rate from aqueous solution onto the solid biodiesel waste residue. **Bioresource Technology**, v. 148, n. , p. 550-559, 2013.
- SIMATUPANG, M.; LANGE, H.; KASIM, A., SEDDING, N. Influence of wood species on the setting of cement and gypsum, in: A.H. Moslemi, MP (Ed.) Fibre and particleboards bonded with inorganic binders. **Forest Products and Research Society**, Madison (WI), 1989, pp. 33-42.
- SIMATUPANG, M.; LANGE, H.; KASIM, A.; SEDDING, N. Influence of wood species on the setting of cement and gypsum, in: A.H. Moslemi, MP (Ed.) Fibre and particleboards bonded with inorganic binders, **Forest Products and Research Society**, Madison (WI), 1989, pp. 33-42.
- SINGH, S. Investigations into the causes of poor strength of portland cement bonded lignocellulosic materials. **Journal of the Indian Academy of Wood Science**, v. 17, n. 10, p. 15-19, 1979.
- T.TAPPI, 204 cm-97, Solvent extractives of wood and pulp, TAPPI test methods, 2004.
- T.TAPPI, 211 om-16, Ash in wood, pulp, paper and paperboard: combustion at 525°C, TAPPI test methods, 2009.
- T.TAPPI, 222 om-98, Modified procedure to determine acid-insoluble lignin in wood and pulp, TAPPI test methods, 1998.
- TAKAHASHI, T. A feature of linen and ramie, **Sen'i Gakkaishi** (in Japanese), v. 42, n. 4, p. 319-321, 1986.
- VAICKELIONIS, G.; VAICKELIONIENE, R. Cement hydration in the presence of wood extractives and pozzolan mineral additives. **Ceramics-Silikaty**, v. 50, n. 2, p. 115-122, 2006.
- WANG, J.; WAN, W. Optimization of fermentative hydrogen production process using genetic algorithm based on neural network and response surface methodology, **International Journal of Hydrogen Energy**, v. 34, n. , p. 255-261, 2009.
- WATANABE, K.; KORAI, H.; MATSUSHITA, Y.; HAYASHI, T. Predicting internal bond strength of particleboard under outdoor exposure based on climate data: comparison of multiple linear regression and artificial neural network. **Journal of Wood Science**, v. 61, n.2,p. 151-158, 2015.
- WILLIAM, G. M. C.; COCHRAN, G. **Experimental Designs**, 2nd Edition, J. Willey and Sons, New York, USA, 1992.
- ZHANG, G.; PATUWO, B. E.; HU, M. Y. Forecasting with artificial neural networks: The state of the art. **International Journal of Forecasting**, v. 14, n. 1, p.35-62, 1998.
- ZHENG Tian, L.; MOSLEMI, A. Influence of chemical additives on the hydration characteristics of western larch wood-cement-water mixtures. **Forest Products Journal**, v. 35, p. 37-43, 1985.
- ZHOU, Y.; KAMDEM, D. P. Effect of cement/wood ratio on the properties of cement-bonded particleboard using CCA-treated wood removed from service. **Forest Products Journal**, v. 52, n. 3, p. 77, 2002.